

AIAA 82-4024

# Analytical Control Law for Desirable Aircraft Lateral Handling Qualities

H. Ohta\*

*Nagoya University, Chikusa-ku, Nagoya, Japan*

and

P.N. Nikiforuk† and M.M. Gupta‡

*University of Saskatchewan, Saskatoon, Saskatchewan, Canada*

A model-matching technique is used to synthesize a control law which augments the lateral dynamics of an aircraft. The feedback and feedforward gains are derived in terms of the lateral stability derivatives and the control law is designed to satisfy specified lateral handling criteria. The augmented plant has specified lateral characteristic poles and a decoupled transfer function matrix between the aileron and rudder angles as inputs and the bank and sideslip angles as outputs. Approximate relationships are derived between the basic and augmented stability derivatives and presented in tabular form. The feedback gains are determined using the augmented derivatives. Simulation examples for three different flight conditions of a STOL aircraft are given to illustrate and substantiate the effectiveness of the control law.

## Nomenclature

$A, B, C$	= coefficient matrices of the plant in Eq. (1)
$F, G, H$	= coefficient matrices of the desirable model
$f_{ij}$	= parameters defined in Eq. (6)
$I$	= unit matrix of appropriate size
$K_\phi, K_\beta$	= sensitivities of the control inputs in Eq. (3)
$L_\mu$	= $m \times m$ matrices defined in Eq. (5)
$L_{(\cdot)}, N_{(\cdot)}, Y_{(\cdot)}$	= dimensional stability derivatives in Eq. (2)
$m$	= number of inputs or outputs
$N_{\delta a}^\phi$	= numerator polynomial in the transfer function $\phi(s)/\delta_a(s)$
$n$	= state dimension of the plant
$p$	= roll rate
$Q$	= gain matrices defined in Eq. (5)
$r$	= yaw rate
$s$	= Laplace operator
$u$	= $m$ -dimensional input vector
$V_0$	= flight velocity
$x$	= state vector
$y$	= $m$ -dimensional output vector
$\beta$	= sideslip angle
$\gamma_0$	= glide path angle
$\Delta_{lat}$	= characteristic polynomial of the lateral dynamics
$\delta$	= control surface deflection
$\zeta$	= damping ratio
$\tau$	= time constant
$\phi$	= bank angle
$\omega$	= natural frequency

## Superscripts

$T$	= matrix or vector transpose
$-1$	= inverse of a matrix

## Subscripts

$a$	= aileron
$d$	= dutch roll
$m$	= model
$p$	= plant or roll rate
$r$	= yaw rate, rudder, or roll mode

$s$	= spiral mode
$\beta$	= sideslip angle
$\phi$	= bank angle

## Introduction

THE implicit model-following method has several advantages over the explicit model-following method for the design of stability and control augmentation systems (SCAS) for aircraft.<sup>1,2</sup> These advantages include the fact that the derived control law is simpler and the feedback gains are smaller. The compensator is also less complex since it does not require implementation of a "desirable model," which avoids errors due to the initial conditions of the compensator. In addition, the characteristic roots of the plant may be placed nearer to those of the model, giving the augmented plant a better gust response.<sup>1</sup> Neither method, however, can directly incorporate the criteria for the lateral handling qualities in the augmented responses of the plant because of the use of a quadratic performance index of the output errors and inputs. The situation becomes worse when weighting matrices are interposed into the index. Consequently, acceptable results can usually be obtained only after completing a computer simulation.

For the solution of these problems, the authors had previously discussed a model-matching technique,<sup>3</sup> which is more closely related to an implicit model-following method than an explicit one, and they have derived explicit feedback laws using a simplified set of lateral dynamics for the aircraft. The design specifications, however, are directly achieved in the model-matching method, since the main requirement is that of finding a controller that forces the plant to follow the desirable model in an input-output sense. In this paper, the results given previously<sup>3</sup> are extended and verified. In particular, the following points are discussed:

1) Feedback and feedforward gains are based on linearized equations of the lateral dynamics. In particular, the derivatives  $L'_r$  and  $N'_p$ , previously neglected, are retained and equations are derived explicitly in terms of the stability derivatives.

2) Approximate equations for these control gains and the augmented stability derivatives are given and their effects on the lateral stability and control characteristics are examined.

Simulation examples for three different flight conditions of a STOL aircraft are then presented to illustrate and substantiate the following: 1) the effect of simplifying the aircraft dynamics; 2) the output tracking characteristics of the augmented plant; 3) the pole-zero assignments of the

Received Sept. 8, 1980; revision received March 23, 1981. Copyright © American Institute of Aeronautics and Astronautics, Inc., 1981. All rights reserved.

\*Lecturer, Dept. of Aeronautical Engineering. Member AIAA.

†Dean and Professor, Cybernetics Research Laboratory.

‡Professor, Cybernetics Research Laboratory.

augmented plant to their desirable locations; 4) the accuracy of the approximate control gains and the augmented stability derivatives; and 5) the sensitivities of the control gains to the parameter variations of the plant.

It is assumed in this paper, as in any explicit and implicit model-following method, that all of the states of the plant are measurable and that a state observer<sup>4</sup> can be used, if necessary, to construct the estimates of the states.

### Aircraft Dynamics and Desirable Model

The aircraft lateral dynamics which are to be controlled are essentially the same as those given in Ref. 3 and are reproduced here for convenience:

$$\dot{x}_p = Ax_p + Bu_p \quad y_p = Cx_p \quad (1)$$

where the state, input, and output vectors of the plant are

$$x_p^T = [p \phi r \beta] \quad u_p^T = [\delta_a \delta_r] \quad y_p^T = [\phi \beta]$$

The coefficient matrices  $A$ ,  $B$ , and  $C$  are given by

$$A = \begin{bmatrix} L'_p & 0 & L'_r & L'_\beta \\ 1 & 0 & 0 & 0 \\ N'_p & 0 & N'_r & N'_\beta \\ Y_p^* & Y_\phi^* & Y_r^* - 1 & Y_\beta^* \end{bmatrix} \quad B = \begin{bmatrix} L'_{\delta a} & L'_{\delta r} \\ 0 & 0 \\ N'_{\delta a} & N'_{\delta r} \\ Y_{\delta a}^* & Y_{\delta r}^* \end{bmatrix} \quad (2)$$

$$C = \begin{bmatrix} 0 & 1 & 0 & 0 \\ 0 & 0 & 0 & 1 \end{bmatrix}$$

$$Q = \tilde{Q} + L_\mu \hat{Q} \quad \Delta = L_{\delta a} N_{\delta r} - L_{\delta r} N_{\delta a}$$

$$\tilde{Q} = \frac{1}{\Delta} \begin{bmatrix} -N_{\delta r} L_p + L_{\delta r} (N_p - Y_\phi) & -L_{\delta r} Y_\phi Y_\beta \\ N_{\delta a} L_p - L_{\delta a} (N_p - Y_\phi) & L_{\delta a} Y_\phi Y_\beta \end{bmatrix}$$

$$\hat{Q} = \frac{1}{\Delta} \begin{bmatrix} -N_{\delta r} f_{21} & -(N_{\delta r} f_{11} + L_{\delta r} Y_\phi f_{21}) \\ N_{\delta a} f_{22} & (N_{\delta a} f_{12} + L_{\delta a} Y_\phi f_{22}) \end{bmatrix}$$

In the following analysis, it will be assumed that the stability derivatives  $Y_p^*$ ,  $Y_r^*$ ,  $Y_{\delta a}^*$  are small and may be neglected.<sup>3</sup> In addition, the derivative  $Y_{\delta r}^*$  will also be neglected.<sup>§</sup> These simplifications will be examined later. However, the derivatives  $L'_r$  and  $N'_p$ , which were neglected in Ref. 3, are retained in the dynamic equations in order to provide a more realistic dynamic model of the aircraft. In addition, in the following work the primes and asterisks on the stability derivatives are dropped for convenience and the desirable model is selected on the basis of the following handling qualities<sup>5</sup>: 1) poles of the roll, spiral, and dutch roll modes are located at specified positions; 2) numerator-to-denominator frequency ratio of the dutch roll mode,  $\omega_\phi/\omega_d$ , is approximately unity, which means that the roll-yaw coupling characteristics are good; 3) ratio of the bank angle to the sideslip angle of the dutch roll mode  $|\phi/\beta|_d$  is small, which alleviates the gust response; 4) sideslip angle  $\beta$  is minimized, which yields good coordinated-turn characteristics; and 5) control effectiveness is selected to achieve a given set of values.

These requirements are realized by means of a decoupled transfer function matrix<sup>3</sup> which represents the desirable

model. Its diagonal components  $\phi_m(s)/\delta_{am}(s)$  and  $\beta_m(s)/\delta_{rm}(s)$  are given by

$$\begin{aligned} \phi_m(s)/\delta_{am}(s) &= K_\phi / (s + 1/\tau_s)(s + 1/\tau_r) \\ \beta_m(s)/\delta_{rm}(s) &= K_\beta / (s^2 + 2\zeta_d \omega_d s + \omega_d^2) \end{aligned} \quad (3)$$

where  $K_\phi$  and  $K_\beta$  are the control effectiveness and  $\tau_s, \tau_r, \zeta_d$ , and  $\omega_d$  are the spiral time constant, roll time constant, dutch roll damping, and natural frequency, respectively. The values of these constants are to be selected by the designer according to some desired handling qualities of the aircraft.

### Analytical Control Law and Augmented Stability Derivatives

The model-matching method, which is used to derive the control law, is described in Ref. 3. It has the following restrictions applied to it. The dimensions of the plant and model inputs and outputs must be of the same order, and the triplets  $(A, B, C)$  and  $(F, G, H)$  of the plant and the model must be completely controllable and observable. In addition,  $\text{Num det } C(sI - A)^{-1}B$  must have no zeros in the right-hand side of the  $s$  plane,<sup>¶</sup> where

$$\text{Num det } C(sI - A)^{-1}B \triangleq \text{det } C(sI - A)^{-1}B \cdot \text{det } (sI - A)$$

The control law derived using the model-matching algorithm is given by

$$u_p = Qx_p + L_\mu u_m \quad (4)$$

where  $u_m^T = [\delta_{am}, \delta_{rm}]$  is the vector of the reference aileron and rudder control inputs to the augmented plant. The gain matrices  $Q$  and  $L_\mu$  are given by

$$L_\mu = \frac{1}{\Delta} \begin{bmatrix} K_\phi N_{\delta r} & K_\beta L_{\delta r} \\ -K_\phi N_{\delta a} & -K_\beta L_{\delta a} \end{bmatrix}$$

$$\begin{bmatrix} L_{\delta r} (N_r + Y_\beta) - L_r N_{\delta r} & -N_{\delta r} L_\beta + L_{\delta r} (N_\beta - Y_\beta^2) \\ -L_{\delta a} (N_r + Y_\beta) + L_r N_{\delta a} & N_{\delta a} L_\beta - L_{\delta a} (N_\beta - Y_\beta^2) \end{bmatrix}$$

$$\begin{bmatrix} L_{\delta r} f_{21} & -L_{\delta r} (f_{11} + Y_\beta f_{21}) \\ -L_{\delta a} f_{22} & L_{\delta a} (f_{12} + Y_\beta f_{22}) \end{bmatrix} \quad (5)$$

where the coefficients  $f_{ij}$  are determined by the desirable location of the poles and are defined by

$$f_{11} = 1/\tau_s \tau_r \quad f_{21} = 1/\tau_s + 1/\tau_r \quad f_{12} = \omega_d^2 \quad f_{22} = 2\zeta_d \omega_d \quad (6)$$

Using the control law of Eq. (4), the matrices of the plant  $A$  and  $B$  are augmented, respectively, to  $A + BQ$  and  $BL_\mu$  in the closed-loop system. The first term  $\tilde{Q}$  of the feedback gain  $Q$  is the one that shifts all the characteristic roots of the plant to the origin of the  $s$  plane. This can be confirmed by calculating the poles of the matrix  $A + B\tilde{Q}$ . The factor  $\hat{Q}$  of the second term moves the poles from the origin to the specified locations. The feedback gain  $L_\mu$ , on the other hand, is used for adjusting the control sensitivities and eliminating their coupling. The driving matrix  $B$  conveys the pilot's commands and in the closed-loop system is

$$(BL_\mu)^T = \begin{bmatrix} K_\phi & 0 & 0 & 0 \\ 0 & 0 & -K_\beta & 0 \end{bmatrix} \quad (7)$$

To determine how the stability derivatives in the matrix  $A$  are affected by the control law, explicit and simple ex-

<sup>§</sup>Stengel<sup>8</sup> has recently worked on the same dynamic equations for horizontal flight conditions.

<sup>¶</sup>This restriction is imposed to assure the stability of the compensator.

Table 1 Approximate augmented stability derivatives

Stability derivatives	Augmented stability derivatives
$L_p, L_r$	$-\frac{K_\phi}{L_{\delta a}} f_{21}, \frac{K_\phi L_{\delta r}}{L_{\delta a} N_{\delta r}} f_{21}$
$L_\phi$	$-\frac{K_\phi}{L_{\delta a}} \left( f_{11} + \frac{L_{\delta r}}{N_{\delta r}} Y_\phi f_{21} \right)$
$L_\beta$	$-\frac{K_\phi L_{\delta r}}{L_{\delta a} N_{\delta r}} (f_{11} + Y_\beta f_{21})$
$N_p, N_r$	$-\frac{K_\beta N_{\delta a}}{L_{\delta a} N_{\delta r}} f_{22} + Y_\phi, \frac{K_\beta}{N_{\delta r}} f_{22} - Y_\beta$
$N_\phi$	$-\frac{K_\beta}{N_{\delta r}} \left( Y_\phi f_{22} + \frac{N_{\delta a}}{L_{\delta a}} f_{12} \right) + Y_\phi Y_\beta$
$N_\beta$	$-\frac{K_\beta}{N_{\delta r}} (f_{12} + Y_\beta f_{22}) + Y_\beta^2$
$Y_p, Y_\phi$ $Y_r, Y_\beta$	$\left. \begin{array}{l} Y_{j \text{ aug}} = Y_j + Y_{\delta r} q_{2j} \\ Q = [q_{ij}] \quad (i=1,2; j=p,\phi,r,\beta) \end{array} \right\}$
$L_{\delta a}, L_{\delta r}$	$K_\phi, 0$
$N_{\delta a}, N_{\delta r}$	$0, -K_\beta$
$Y_{\delta a}, Y_{\delta r}$	$-\frac{K_\phi N_{\delta a}}{L_{\delta a} N_{\delta r}} Y_{\delta r}, -\frac{K_\beta}{N_{\delta r}} Y_{\delta r}$

pressions which describe the elements of the matrix  $A+BQ$  will now be sought. For this purpose, the augmented derivatives are calculated assuming that in Eq. (5),

$$\Delta \approx L_{\delta a} N_{\delta r} \quad \text{for} \quad \left| \frac{L_{\delta r} N_{\delta a}}{L_{\delta a} N_{\delta r}} \right| \ll 1 \quad (8)$$

This approximation is sufficiently accurate for conventional aircraft. Table 1 shows the approximate augmented stability derivatives which are denoted by  $(\cdot)_{\text{aug}}$ . It is to be noted that  $L_{\phi \text{ aug}}$  and  $N_{\phi \text{ aug}}$ , which are the zeros in the original equations, appear when augmented. The effects of  $Y_{\delta r}$  on the augmented derivatives, which were neglected in the derivation of the control law, are also given in the table. Each  $Y$  derivative in the bottom row of  $A$  varies by the value of the corresponding element of the second row of the matrix  $Q$  multiplied by  $Y_{\delta r}$ . The value of  $Y_{\delta r}$ , however, is small (usually of the order of  $10^{-2}$ ) and has little effect on the closed-loop system. Should the control law be derived without neglecting  $Y_{\delta r}$ , it would be more complex with dynamic compensation.<sup>3</sup>

Using Eq (8), the approximate feedback and feedforward gains in Eq. (5) are determined in terms of the augmented derivatives given in Table 1:

$$L_\mu \approx \begin{bmatrix} K_\phi / L_{\delta a} & k_\beta E_r / L_{\delta r} \\ -K_\phi E_a / N_{\delta r} & -K_\beta / N_{\delta r} \end{bmatrix}$$

$Q =$

$$\begin{bmatrix} \frac{1}{L_{\delta a}} [L_{p \text{ aug}} - L_p - E_r (N_{p \text{ aug}} - N_p)] & \frac{1}{L_{\delta a}} [L_{\phi \text{ aug}} - E_r N_{\phi \text{ aug}}] & \frac{1}{L_{\delta a}} [L_{r \text{ aug}} - L_r - E_r (N_{r \text{ aug}} - N_r)] & \frac{1}{L_{\delta a}} [L_{\beta \text{ aug}} - L_\beta - E_r (N_{\beta \text{ aug}} - N_\beta)] \\ \frac{1}{N_{\delta r}} [N_{p \text{ aug}} - N_p - E_a (L_{p \text{ aug}} - L_p)] & \frac{1}{N_{\delta r}} [N_{\phi \text{ aug}} - E_a L_{\phi \text{ aug}}] & \frac{1}{N_{\delta r}} [N_{r \text{ aug}} - N_r - E_a (L_{r \text{ aug}} - L_r)] & \frac{1}{N_{\delta r}} [N_{\beta \text{ aug}} - N_\beta - E_a (L_{\beta \text{ aug}} - L_\beta)] \end{bmatrix} \quad (9)$$

where  $E_a = N_{\delta a} / L_{\delta a}$  and  $E_r = L_{\delta r} / N_{\delta r}$ . The gains  $Q$  and  $L_\mu$  in Eq. (9) from now on will be called the approximate gains of Eq. (5).

### Numerical Example and Discussion of Results

Some simulation studies were conducted to verify the control law given in Eqs. (4) and (5), their approximate gains in Eq. (9), and the augmented stability derivatives in Table 1. The main points of concern are those five discussed in the Introduction. For this purpose a numerical example of a STOL aircraft was taken from Hartmann.<sup>6</sup> Three flight conditions were investigated (FC Nos. 1 to 3) and are described in Table 2. The values of the basic stability derivatives are given in Table 3. It is desired that the augmented dynamics for each flight condition exhibit the desired transfer functions of Eq. (3), whose characteristics poles are determined to be

$$1/\tau_r = 2.5 \quad 1/\tau_s = 0.02 \quad \zeta_d = 0.7 \quad \omega_d = 2.3 \quad (10)$$

### Effects of Simplifying the Controlled Dynamics

To illustrate the effects of simplifying the aircraft dynamics, two time histories, one with simplified dynamics and the other with complete dynamics, are presented in Figs. 1a and 2a for FC No. 2. Figure 1a gives the responses of the unaugmented aircraft to a 3-deg rectangular pulse aileron input  $\delta_{am}$  of 1-s duration (an "impulse") and Fig. 2a gives the responses to a 3-deg step rudder input  $\delta_{rm}$ . These figures show that neglecting  $Y_p, Y_r, Y_{\delta a}$ , and  $Y_{\delta r}$  in the dynamics does not produce a significant difference between the two time histories. These figures also show the problems caused by the deficient dutch roll and the spiral instability of the controlled plant. The desirable responses  $\phi_m$  and  $\beta_m$  are also shown in the figures. They are achieved by a control law that matches  $\phi$  with  $\phi_m$ , while keeping  $\beta$  close to zero in Fig. 1a, and  $\beta$  with  $\beta_m$ , while keeping  $\phi$  close to zero in Fig. 2a.

### Tracking Performance

The responses of the augmented aircraft described by the control law in Eqs. (4) and (5), and shown in Figs. 1b and 2b, exhibit good tracking and decoupled performances. Figures 3a and 3b illustrate the unaugmented and augmented responses to a 3-deg  $\delta_{rm}$  input for FC No. 1. It is seen that the unaugmented response of  $\phi$  diverges to more than 20 deg in 10 s, and that it is suppressed to about 2 deg after augmentation. The control magnitudes are within 3 deg. In these calculations the control sensitivities,  $K_\phi$  and  $K_\beta$ , were selected such that the diagonal elements of the feedforward gain  $L_\mu$  in Eq. (5) are equal to unity. The control gains for each flight condition are given in Table 4. This table also shows the approximate values that were obtained using Eq. (9), where  $K_\phi = L_{\delta a}$  and  $K_\beta = -N_{\delta r}$  were selected. This selection makes the values of the diagonal elements of  $L_\mu$  equal to unity, which implies that the control effectiveness of the augmented plant is equivalent to that of the basic aircraft. It is confirmed in Table 4 that the approximation of Eq. (9) to Eq. (5) is excellent.

### Accuracy of the Augmented Stability Derivatives

Two kinds of augmented stability derivatives are shown in Table 3. The one termed "complete" was obtained from the closed-loop system, where the exact control gains, Eq. (5), were used in the complete dynamic equations. The other, termed "approximate," was calculated using Table 1. Both sets show good agreement.

Table 2 Flight conditions of the STOL aircraft used for numerical example

FC No.	Flight condition	Mass, kg	Altitude, m	Forward velocity $V_0$ , m/s	Flap position, deg	Glide path angle $\gamma_0$ , deg	Dynamic pressure $q_D$ , N/m <sup>2</sup>
1	Cruise, fully loaded	3500	2000	77.8	0	0	3046
2	Descent	3400	0	33.4	20	-5.4	683
3	Steep descent	3500	0	30.9	52	-10.4	585

Table 3 Stability derivatives<sup>a</sup> of the basic and augmented aircraft

Stability derivatives	FC No. 1			FC No. 2			FC No. 3		
	Unaugmented dynamics	Augmented dynamics		Unaugmented dynamics	Augmented dynamics		Unaugmented dynamics	Augmented dynamics	
		Complete (Eq. 5)	Approximate (Table 1)		Complete (Eq. 5)	Approximate (Table 1)		Complete (Eq. 5)	Approximate (Table 1)
$L_p$	-5.247	-2.520		-2.670	-2.520		-2.488	-2.520	
$L_\phi$	0.0	0.2019		0.0	0.0420		0.0	0.1694	
$L_r$	1.190	-1.999		2.050	-0.3149		2.299	-0.7034	
$L_\beta$	-8.830	-0.4049	Same as the left column	-1.304	-0.0282	Same as the left column	-1.216	0.0553	Same as the left column
$N_p$	-0.0341	0.0839		-0.1558	0.5188		0.2383	0.4782	
$N_\phi$	0.0	0.3085		0.0	1.281		0.0	1.247	
$N_r$	-1.406	-2.998		-0.7450	-3.111		-0.6716	-3.122	
$N_\beta$	5.673	4.623		1.829	4.949		1.644	4.983	
$Y_p$	-0.0024	-0.0045	-0.0045	0.0	-0.0202	-0.0204	-0.0005	-0.0233	-0.0237
$Y_\phi$	0.1260	0.1219	0.1219	0.2921	0.2532	0.2529	-0.3119	0.2726	0.2720
$Y_r$	0.0131	0.0349	0.0347	0.0134	0.0804	0.0809	0.0131	0.0859	0.0870
$Y_\beta$	-0.2224	-0.2099	-0.2100	-0.1095	-0.2017	-0.2025	-0.0984	-0.2026	-0.2041
$L_{\delta a}$	15.120	14.963	15.120	3.356	3.386	3.356	2.887	2.929	2.887
$L_{\delta r}$	4.891	0.0	0.0	0.1426	0.0	0.0	0.2728	0.0	0.0
$N_{\delta a}$	-0.1979	0.0	0.0	0.2363	0.0	0.0	0.1491	0.0	0.0
$N_{\delta r}$	-6.166	-6.102	-6.166	-1.141	-1.151	-1.141	-0.9774	-0.9915	-0.9774
$Y_{\delta a}$	0.0	-0.0026	-0.0026	0.0	0.0073	0.0073	0.0	0.0048	0.0048
$Y_{\delta r}$	0.0814	0.0814	0.0814	0.0350	0.0350	0.0350	0.0315	0.0315	0.0315

<sup>a</sup> The derivatives are so-called primed ones<sup>3</sup> and the dimensions correspond to Ref. 7.

Table 3 also shows the augmented characteristics of the aircraft. The roll damping  $L_p$  represents  $-(1/\tau_r + 1/\tau_s)$ . The dihedral effect  $L_\beta$  is changed to a small negative value, and contributes to the dutch roll damping. The yaw damping  $N_r$ , the main contributor to the dutch roll damping, becomes approximately equal to  $-2\zeta_d\omega_d$ . The weathercock stability  $N_\beta$  determines the natural frequency of the dutch roll mode, and is approximately equal to  $\omega_d^2$ . On the other hand, the control effectivenesses,  $L_{\delta a}$  and  $N_{\delta r}$ , remain unchanged due to the selection of  $K_\phi$  and  $K_\beta$  mentioned previously. The cross-effectiveness derivatives,  $L_{\delta r}$  and  $N_{\delta a}$ , become equal to zeros. The derivatives  $Y_p$ ,  $Y_r$ ,  $Y_{\delta a}$ , and  $Y_{\delta r}$  remain small, which verifies the assumption that was made earlier.

#### Handling Qualities

Design specifications 3 and 4 that were used for selecting the desirable model will now be discussed. In the conventional, single-loop feedback control the feedback of  $p$  to  $\delta_a$ , referred to as the roll damper, augments  $L_p$  and improves both  $1/\tau_r$  and the roll-gust response. One of the criteria of the roll response to a side-gust input is the amplitude ratio

$$\left| \frac{\phi}{\beta} \right|_d = \left| \frac{L_\beta}{N_\beta} \right| \frac{1}{\sqrt{1 + L_\beta^2/N_\beta^2}} \quad (11)$$

for the dutch roll mode.<sup>7</sup> Evaluating Eq. (11) using the augmented stability derivatives from Table 3,  $|\phi/\beta|_d$  of the augmented airplane is found to be less than one tenth that of the basic airplane for each flight condition. This is due to a

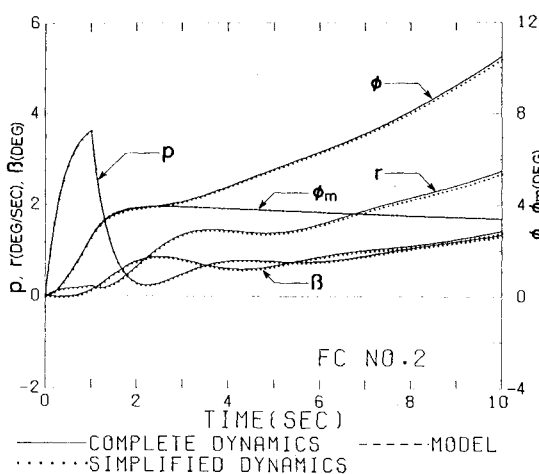
large decrease of  $L_{\beta\text{aug}}$  compared to  $L_\beta$ . On the other hand, the requirement of minimizing the  $\beta$  response is realized by the feedback of  $\beta$  and  $\dot{\beta}$  to  $\delta_r$  for the single-loop control, whose feedbacks compensate and increase  $N_\beta$ . The values of  $N_{\beta\text{aug}}$  in Table 3 are increased for FC Nos. 2 and 3, but are decreased for FC No. 1. This is due to a compromise between good coordinate-turn characteristics and the gust response.

#### Pole-Zero Assignment

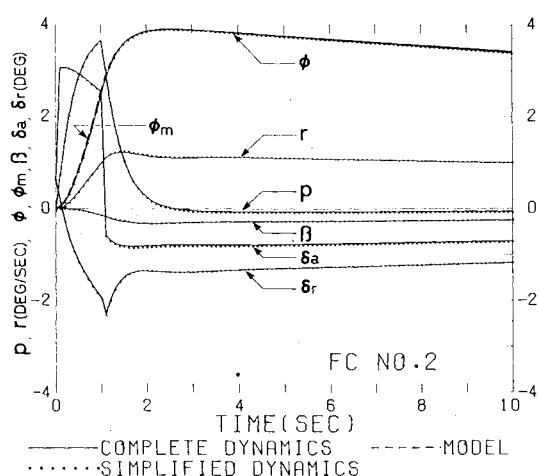
The transfer functions of the open- and closed-loop systems are compared in Table 5. It shows that the closed-loop system coincides with the desired transfer function of the model even though the small stability derivatives are neglected and the control gains are simplified; that is, the characteristic poles coincide with those in Eq. (10). The dutch roll mode is cancelled in  $N_{\delta a}^\phi(s)$ , while the spiral and the roll modes are cancelled in  $N_{\delta r}^\beta(s)$ .

#### Sensitivity Considerations

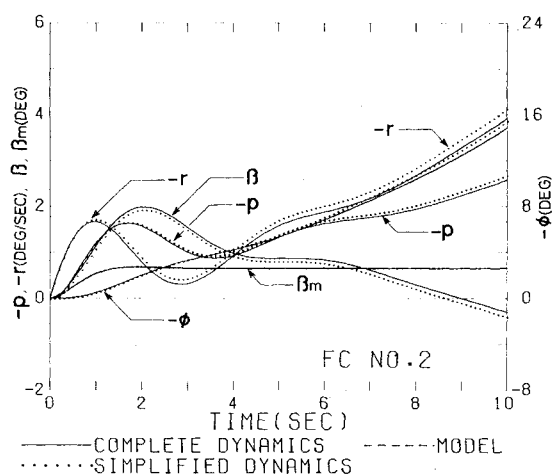
To examine the sensitivity of the control gains to the plant parameter variations, the aircraft flying under FC No. 3 was controlled using the control gains that were calculated for FC No. 2. The time histories of the basic aircraft for FC No. 3, which are not presented, exhibit more severe spiral instability than those for FC No. 2 (Figs. 1a and 2a). Figures 4a and 4b illustrate the augmented responses, where the solid lines represent the responses for the correct values of the gains and the dotted lines for the gain values of FC No. 2. These figures indicate a slight spiral instability. Feedback gains that con-



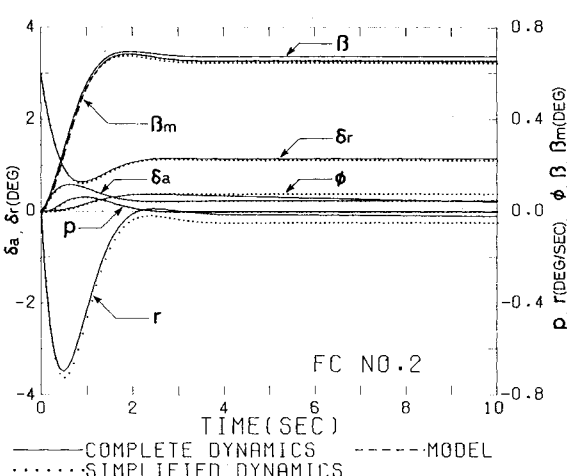
a)



b)



a)



b)

Fig. 1 Response to a three-degree impulse aileron input for FC No. 2: a) unaugmented, b) augmented.

Fig. 2 Responses to a three-degree step rudder input for FC No. 2: a) unaugmented, b) augmented.

Table 4 Feedback and feedforward gains

FC No.	Equation used	$K_\phi, K_\beta$	$L_\mu$	$Q$			
1	Complete	14.963	$\begin{bmatrix} 1.0 & -0.3235 \\ -0.0321 & 1.0 \end{bmatrix}$	$\begin{bmatrix} 0.1885 & 0.0298 & -0.2975 & 0.5074 \\ -0.0252 & -0.0510 & 0.2677 & 0.1540 \end{bmatrix}$			
	Eq. (5)	6.102					
	Approximate <sup>a</sup>	15.120	Same as above	$\begin{bmatrix} 0.1883 & 0.0292 & -0.2913 & 0.4999 \\ -0.0251 & -0.0499 & 0.2594 & 0.1601 \end{bmatrix}$			
	Eq. (9)	6.166					
2	Complete	3.386	$\begin{bmatrix} 1.0 & -0.0425 \\ 0.2071 & 1.0 \end{bmatrix}$	$\begin{bmatrix} 0.0692 & 0.0597 & -0.7859 & 0.4920 \\ -0.5769 & -1.1100 & 1.9100 & -2.6330 \end{bmatrix}$			
	Eq. (5)	1.151					
	Approximate <sup>a</sup>	3.356	Same as above	$\begin{bmatrix} 0.0633 & 0.0608 & -0.7947 & 0.4979 \\ -0.5851 & -1.1310 & 1.9520 & -2.6940 \end{bmatrix}$			
	Eq. (9)	1.141					
3	Complete	2.929	$\begin{bmatrix} 1.0 & -0.0945 \\ 0.1526 & 1.0 \end{bmatrix}$	$\begin{bmatrix} 0.0574 & 0.1767 & -1.2590 & 0.7145 \\ -0.7243 & -1.2490 & 2.3150 & -3.3070 \end{bmatrix}$			
	Eq. (5)	0.992					
	Approximate <sup>a</sup>	2.887	Same as above	$\begin{bmatrix} 0.0460 & 0.1818 & -1.2850 & 0.7315 \\ -0.7391 & -1.2850 & 2.3950 & -3.4290 \end{bmatrix}$			
	Eq. (9)	0.977					

<sup>a</sup>  $K_\phi = L_{\delta a}$ ,  $K_\beta = -N_{\delta r}$ ,  $L_\mu = \begin{bmatrix} 1.0 & -L_{\delta r}/L_{\delta a} \\ -N_{\delta a}/N_{\delta r} & 1.0 \end{bmatrix}$

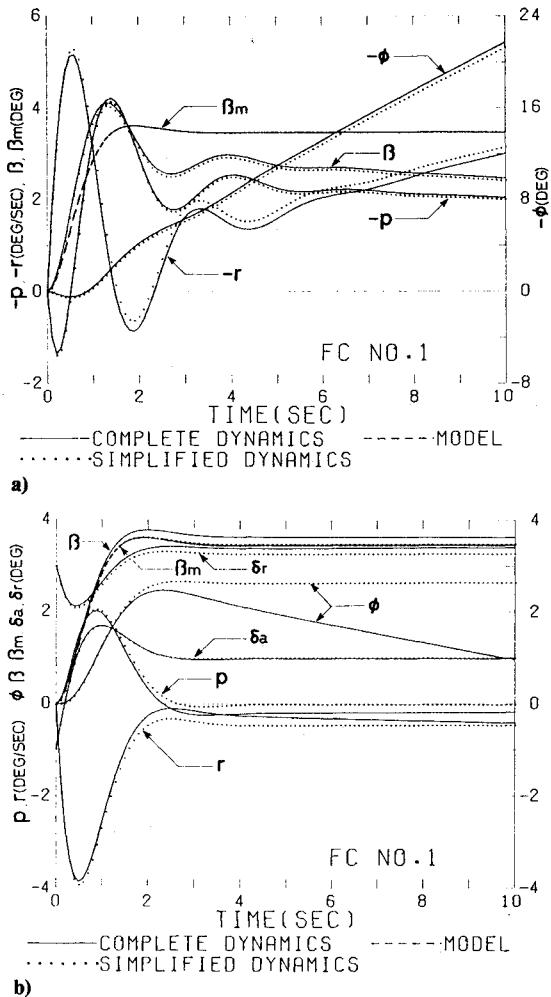


Fig. 3 Responses to a three-degree step rudder input for FC No. 1: a) unaugmented, b) augmented.

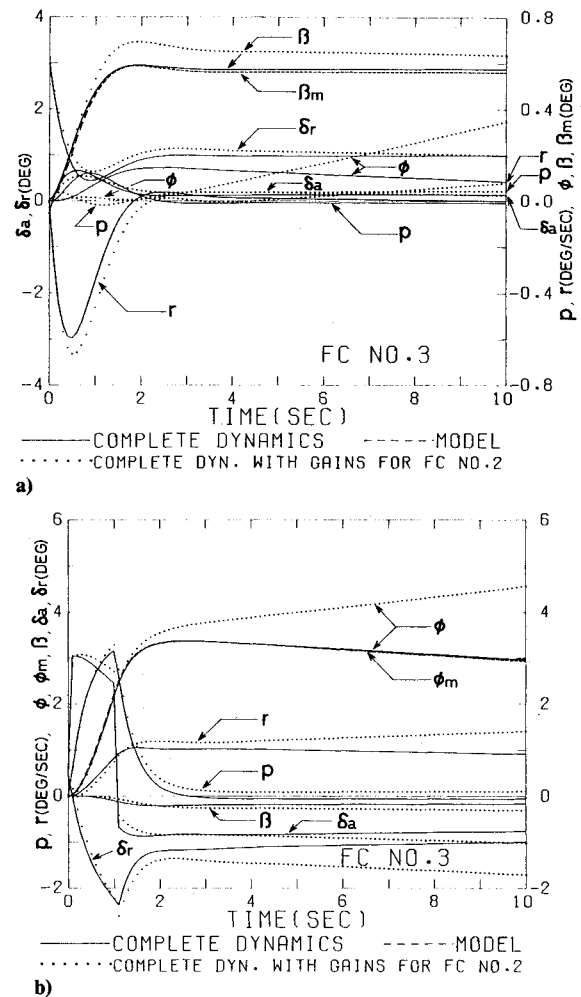


Fig. 4 Augmented responses to a) three-degree impulse aileron input and b) three-degree step rudder input for FC No. 3.

Table 5 Transfer functions of the open- and closed-loop systems (poles of the model:  $1/\tau_r = 2.500$ ,  $1/\tau_s = 0.020$ ,  $s_d = -1.610 \pm 1.643j$ )

FC No.	Transfer function	Open loop		Closed loop	
		Complete dynamics	Simplified dynamics complete Eq. (5)	Complete Eq. (5)	Approximate Eq. (9)
1	$\Delta_{lat}$	$-5.293, -0.0222$ $-0.780 \pm 2.336j$	$-2.521, -0.0200$ $-1.600 \pm 1.623j$	$-2.509, -0.0204$ $-1.599 \pm 1.562j$	$-2.509, -0.0204$ $-1.599 \pm 1.563j$
	$N_{\delta_a}^{\phi}$	$-0.806 \pm 2.268j$	$-1.610 \pm 1.643j$	$-1.604 \pm 1.588j$	$-1.604 \pm 1.588j$
	$N_{\delta_r}^{\phi}$	$2.355, -2.336$	$-0.0198$	$0.0556$	$0.0548$
	$N_{\delta_a}^{\beta}$	$-0.813, -20.586$	$-1.643$	$-1.887, 5.824$ $-35.200$	$-1.886, 5.862$ $-35.384$
	$N_{\delta_r}^{\beta}$	$-5.396, 0.0017$ $-75.829$	$-2.500, -0.0200$	$-2.490, -0.0195$ $-75.316$	$-2.490, -0.0196$ $-76.092$
2	$\Delta_{lat}$	$-2.679, 0.129$ $-0.487 \pm 1.453j$	$-2.483, -0.0200$ $-1.619 \pm 1.660j$	$-2.475, -0.0190$ $-1.669 \pm 1.577j$	$-2.474, -0.0190$ $-1.670 \pm 1.577j$
	$N_{\delta_a}^{\phi}$	$-0.499 \pm 1.320j$	$-1.610 \pm 1.643j$	$-1.656 \pm 1.560j$	$-1.657 \pm 1.559j$
	$N_{\delta_r}^{\phi}$	$16.448, -0.579$	$-0.198$	$0.0400$	$0.0405$
	$N_{\delta_a}^{\beta}$	$-0.819, 4.567$	$-1.643$	$-1.547, -8.495$ $13.843$	$-1.547, -8.456$ $13.803$
	$N_{\delta_r}^{\beta}$	$-2.952, 0.192$ $-32.790$	$-2.500, -0.0200$	$-2.496, -0.0195$ $-33.333$	$-2.496, -0.0195$ $-33.051$
3	$\Delta_{lat}$	$-2.447, 0.163$ $-0.487 \pm 1.445j$	$-2.472, -0.0200$ $-1.624 \pm 1.670j$	$-2.449, -0.0182$ $-1.688 \pm 1.582j$	$-2.449, -0.0181$ $-1.689 \pm 1.581j$
	$N_{\delta_a}^{\phi}$	$-0.444 \pm 1.251j$	$-1.610 \pm 1.643j$	$-1.662 \pm 1.555j$	$-1.663 \pm 1.554j$
	$N_{\delta_r}^{\phi}$	$7.993, -0.385$	$-0.0198$	$0.0354$	$0.0362$
	$N_{\delta_a}^{\beta}$	$-0.550, 8.705$	$-1.643$	$-1.437, -7.131$ $17.146$	$-1.435, -7.076$ $17.084$
	$N_{\delta_r}^{\beta}$	$-2.922, 0.225$ $-31.091$	$-2.500, -0.0200$	$-2.488, -0.0190$ $-31.915$	$-2.487, -0.0190$ $-31.474$

tribute to the stabilization of the spiral mode are those of  $\beta$  and  $r$  to  $\delta_a$  and yaw damper from  $r$  to  $\delta_r$ . It is also noted from Table 4 that these gain values are insufficient by about 30%, 37%, and 20%, respectively, to the correct values for FC No. 3. These responses, however, exhibit improved dutch roll characteristics and a pilot could control the slight instability because its time constant is large compared to the roll time constant. The implementation of a programmed control in such cases would be straightforward because the control gains are given in terms of the lateral stability derivatives.

### Conclusions

An analytical control law was derived for achieving desirable aircraft lateral handling qualities. The approximate equations of the control gains were presented for a set of augmented stability derivatives. Numerical examples were given to substantiate the control law and the approximate equations.

It is believed that the feedback and feedforward gains derived here could furnish designers with a basic estimate of the desirable lateral handling qualities. Direct side-force control may be used as the third input, other than aileron and rudder inputs. Derivation of the control gains using such three control inputs should be of interest for application to control-configured vehicle technologies.

### Acknowledgments

The support of the National Sciences and Engineering Research Council of Canada under Grants A-5625 and A-1080 is acknowledged. Numerical calculations and

illustrations were carried out using the digital computer (FACOM 230-75/M-200) facility in the Computer Center of Nagoya University. The assistance of E. Nikiforuk in the preparation of this paper is also acknowledged.

### References

- <sup>1</sup> Kreindler, E. and Rothschild, D., "Model-Following in Linear-Quadratic Optimization," *AIAA Journal*, Vol. 14, July 1976, pp. 835-842.
- <sup>2</sup> Gran, R., Berman, H., and Rossi, M., "Optimal Digital Flight Control for Advanced Fighter Aircraft," *Journal of Aircraft*, Vol. 14, Jan. 1977, pp. 32-37.
- <sup>3</sup> Ohta, H., Nikiforuk, P.N., and Gupta, M.M., "Design of Desirable Handling Qualities for Aircraft Lateral Dynamics," *Journal of Guidance and Control*, Vol. 2, Jan.-Feb. 1979, pp. 31-39.
- <sup>4</sup> Luenberger, D.G., "An Introduction to Observers," *IEEE Transactions on Automatic Control*, Vol. AC-16, Dec. 1971, pp. 595-602.
- <sup>5</sup> "Flying Qualities of Piloted Airplanes," Military Specification MIL-F-8785B (ASG), U.S. Government Printing Office, Washington, D.C., Aug. 1969.
- <sup>6</sup> Hartmann, U., "Application of Modal Control Theory to the Design of Digital Flight Control Systems," *Advances in Control Systems*, AGARD CP-137, Sept. 1973, pp. 5.1-5.21.
- <sup>7</sup> McRuer, D., Ashkenas, I., and Graham, D., *Aircraft Dynamics and Automatic Control*, Princeton University Press, Princeton, N.J., 1973, Chap. 6.
- <sup>8</sup> Stengel, R.F., "Some Effects of Parameter Variations on the Lateral-Directional Stability of Aircraft," *Journal of Guidance and Control*, Vol. 3, March-April 1980, pp. 124-131.

## *From the AIAA Progress in Astronautics and Aeronautics Series...*

### **ENTRY HEATING AND THERMAL PROTECTION—v. 69**

### **HEAT TRANSFER, THERMAL CONTROL, AND HEAT PIPES—v. 70**

*Edited by Walter B. Olstad, NASA Headquarters*

The era of space exploration and utilization that we are witnessing today could not have become reality without a host of evolutionary and even revolutionary advances in many technical areas. Thermophysics is certainly no exception. In fact, the interdisciplinary field of thermophysics plays a significant role in the life cycle of all space missions from launch, through operation in the space environment, to entry into the atmosphere of Earth or one of Earth's planetary neighbors. Thermal control has been and remains a prime design concern for all spacecraft. Although many noteworthy advances in thermal control technology can be cited, such as advanced thermal coatings, louvered space radiators, low-temperature phase-change material packages, heat pipes and thermal diodes, and computational thermal analysis techniques, new and more challenging problems continue to arise. The prospects are for increased, not diminished, demands on the skill and ingenuity of the thermal control engineer and for continued advancement in those fundamental discipline areas upon which he relies. It is hoped that these volumes will be useful references for those working in these fields who may wish to bring themselves up-to-date in the applications to spacecraft and a guide and inspiration to those who, in the future, will be faced with new and, as yet, unknown design challenges.

*Volume 69—361 pp., 6 × 9, illus., \$22.00 Mem., \$37.50 List*  
*Volume 70—393 pp., 6 × 9, illus., \$22.00 Mem., \$37.50 List*

TO ORDER WRITE: Publications Dept., AIAA, 1290 Avenue of the Americas, New York, N.Y. 10104